Christopher J. Damaren*
Senior Lecturer,
Department of Mechanical Engineering,
University of Canterbury,
Private Bag 4800,
Christchurch, New Zealand

Lan Le-Ngoc
Scientist,
Industrial Research Ltd.,
5 Sheffield Crescent,
PO Box 20-028,
Christchurch, New Zealand

Robust Active Vibration Control of a Bandsaw Blade

An analytical study of a vibrating bandsaw blade is presented. The blade is modeled as a plate translating over simply-supporting guides. Gyroscopic effects due to the blade's axial motion as well as in-plane forces resulting from tensioning and the influence of the cutting force are included in the model. The latter is modeled as a nonconservative follower force on the cutting edge of the blade and shown to be destabilizing. A state-space model is developed which includes the effects of time-varying cutting forces and exogenous disturbances. Feedback control via a collocated force actuator/rate sensor is introduced and recent advances in robust control theory are used develop controllers which achieve robust stability and performance with respect to the time-varying model.

1 Introduction

The problem of unwanted bandsaw vibrations has attracted much attention over the last 30 years. The motivation for these studies is the suppression of unwanted vibrations which detract from the quality and efficiency of the cutting process. Early work modeled the cutting portion of the bandsaw blade as a translating beam and noted the influence of parameter fluctuations on the system stability (Mote and Naguleswaran, 1966; Naguleswaran and Williams, 1968). Since then structural modeling has grown progressively more complete and both bending and torsion have been studied in the context of either beam (Alspaugh, 1967; Soler, 1968) or plate models (Ulsoy and Mote, 1982; Lengoc and McCallion, 1995).

Lehmann and Hutton (1996) have presented a detailed plate model which includes a deflection model for the cutting teeth and the forces involved in contact between the blade and sawn surfaces. This formed the basis for a simulation of the cutting process (Lehmann and Hutton, 1997).

Much of the above work has painted time-varying parameters, especially blade tension, as major culprits in creating system instability. The recent detailed study by Lengoc and McCallion (1995) has suggested another important mechanism for bandsaw destabilization. There, it is shown numerically that a tangential cutting force which follows the deformed shape of the blade can create dynamic instability. This is a specific instance of the flutter phenomenon which originates from a circulatory term in the motion equation.

In the present work, it is shown that relatively simple feedback controllers can be designed which eliminate both instability mechanisms. A performance criterion which enforces vibration suppression and a mathematically rigorous model of system uncertainty encompassing the temporal variation of the blade parameters are established. Controllers are developed using recent advances in robust control theory (Shamma, 1994; Poolla and Tikku, 1995) which yield robust performance, that is satisfaction of the performance criterion and system stabilization for the time-varying system. Although the plant is modeled as linear time-varying, the required controllers are linear time-invariant and can be developed using the well known state-space solutions of Doyle et al. (1989) for an appropriate $\mathcal{H}_\infty$ control problem. Sensor and actuator requirements consist of a single point velocity sensor and a device capable of supplying a normal point force on the moving blade.

2 Equations of Motion

This section is used to formulate the dynamics of the bandsaw blade shown in Fig. 1. The cutting portion is modeled as a plate translating in the x-direction over simply-supporting guides. The discrete-parameter motion equations will be developed by applying the Rayleigh-Ritz technique to the energy expressions developed by Lengoc and McCallion (1995).

The kinetic energy for a translating plate is given by

$$T = \frac{1}{2}\int_0^b \int_0^l \rho h\left[c^2 + \left(\frac{\partial w}{\partial t} + c\,\frac{\partial w}{\partial x}\right)^2\right] dxdy \tag{1}$$

Here, ρ is the mass density, l, b, and h are the xyz-dimensions, c is the translational velocity in the x-direction and $w(x, y, t)$ denotes the distribution of transverse displacements. The xyz-coordinates are fixed and do not move with the blade. The strain energy incurred by small transverse bending of a thin plate is

$$U_b = \frac{1}{2} D \int_0^b \int_0^l \left\{\left(\frac{\partial^2 w}{\partial x^2} + \frac{\partial^2 w}{\partial y^2}\right)^2 + 2(1-\nu)\left[\left(\frac{\partial^2 w}{\partial x \partial y}\right)^2 - \frac{\partial^2 w}{\partial x^2}\frac{\partial^2 w}{\partial y^2}\right]\right\} dxdy \tag{2}$$

where D is the plate rigidity and ν is Poisson's ratio. The in-plane stress distribution creates a strain energy given by

$$U_s = \frac{1}{2}\int_0^b \int_0^l \left[N_x\left(\frac{\partial w}{\partial x}\right)^2 + 2N_{xy}\frac{\partial w}{\partial x}\frac{\partial w}{\partial y} + N_y\left(\frac{\partial w}{\partial y}\right)^2\right] dxdy \tag{3}$$

where $N_x(x, y, t)$ and $N_y(x, y, t)$ are normal stresses and $N_{xy}(x, y, t)$ is the shearing stress in the plane of the plate. The simple model used here models a constant axial tension q_0 and superimposed are the stresses created by a uniformly distributed load along the cutting edge, q_c. Hence

$$N_x = q_0 + \rho h c^2 - q_c\frac{ly}{b^2}\left(2\frac{x}{l} - 1\right), \quad N_{xy} = q_c\left(\frac{y}{b}\right)^2, \quad N_y = 0 \tag{4}$$

These expressions are the simplest polynomial descriptions for the in-plane stress distribution which satisfy the boundary conditions. It has been assumed that a counterweight mechanism is used on the bandsaw's upper pulley to compensate for centripetal acceleration.

*Currently, Associate Professor, University of Toronto, Institute for Aerospace Studies, 4925 Dufferin St., Toronto, ON M3H 5T6, Canada.

Contributed by the Technical Committee on Vibration and Sound for publication in the Journal of Vibration and Acoustics. Manuscript received Aug. 1998; revised Feb. 1999. Associate Technical Editor: B. Yang.

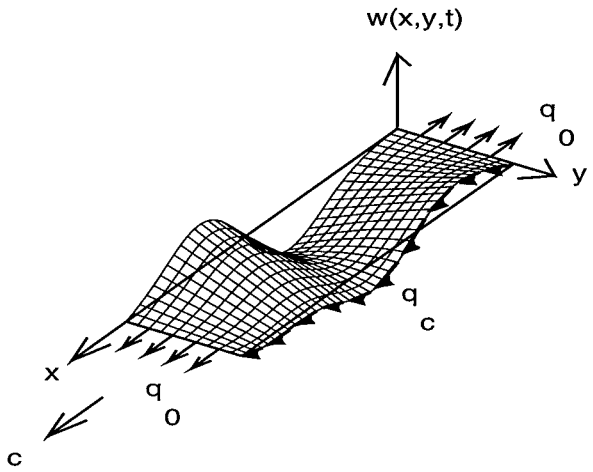

Fig. 1 Bandsaw blade

This is accounted for by the addition of ρhc^2 to the tension in the expression for N_x.

Nonconservative influences stem from the control force, disturbances, and the hypothesis that the cutting force behaves as a follower force on the cutting edge. The virtual work due to these influences is

$$\delta W_{nc} = \int_0^b \int_0^l f_{nc}\delta w dx dy \tag{5}$$

where

$$f_{nc}(x, y, t) = u(t)\delta(x - x_a, y - y_a) + \sqrt{r_w}\sum_{i=1}^{n_d} w_{di}(t)\delta(x - x_{di}, y - y_{di}) + q_f(t)\frac{\partial w}{\partial x}\delta(y - b) \tag{6}$$

The control force $u(t)$ has been modeled as a point load applied at $(x, y) = (x_a, y_a)$ and the $w_{di}(t)$ are disturbances which are modeled in a similar fashion. The latter are largely fictitious and used to enforce performance objectives by exciting the blade along the cutting edge ($y_{di} \equiv b$). They can be thought of as the effect of nonhomogeneities in the material being cut. Their magnitude is scaled using $r_w > 0$. The function $\partial w(x, b)/\partial x$ is the linearized form of the local rotation about the y-axis due to elasticity and $q_f = q_c$. Hence, the last term captures the out-of-plane force created by the follower-force nature of q_c (Fig. 1). The notational independence of q_f from q_c will be maintained so that the follower-force effects can be explicitly exhibited.

The assumed expansion for the plate deflection is

$$w(x, y, t) = \sum_{\alpha=1}^{n}\sum_{\beta=1}^{m} q_{\alpha\beta}(t)\phi_\alpha(x)\psi_\beta(y) \tag{7}$$

where $\phi_\alpha(x) = \sqrt{2/m}\ \sin\ [\alpha\pi x/l]$, $m = \rho lbh$, satisfies the geometric simply-supported conditions at $x = 0$ and $x = l$. Furthermore, they are the exact eigenfunctions for $q_c = q_f = 0$ and cylindrical bending ($\partial w/\partial y = 0$). The ψ_β are the orthogonal polynomials advocated by Bhat (1985). For free-free boundary conditions the first two are $\psi_1(y) = 1$ and $\psi_2(y) = \sqrt{3}\ [2(y/b) - 1]$ and the remaining ones are generated by a Gram-Schmidt type process. These polynomials are, in fact, the classical Legendre polynomials after mapping the interval $[0, b]$ onto $[-1, 1]$. Here, they are normalized such that $\int_0^1 \psi_\alpha(\hat{y})\psi_\beta(\hat{y})d\hat{y} = \delta_{\alpha\beta}$ where $\hat{y} = y/b$.

Substituting the expansion (7) into the energy expressions (1), (2), (3) and (5) gives

$$T = \tfrac{1}{2}[mc^2 + \dot{\mathbf{q}}^T\mathbf{M}\dot{\mathbf{q}} + c\dot{\mathbf{q}}^T\hat{\mathbf{G}}\mathbf{q} + \rho hc^2\mathbf{q}^T\hat{\mathbf{K}}_0\mathbf{q}] \tag{8}$$

$$U_b = \tfrac{1}{2}\mathbf{q}^T\mathbf{K}_b\mathbf{q} \tag{9}$$

$$U_s = \tfrac{1}{2}[(q_0 + \rho hc^2)\mathbf{q}^T\hat{\mathbf{K}}_0\mathbf{q} + q_c\mathbf{q}^T\hat{\mathbf{K}}_c\mathbf{q}] \tag{10}$$

$$\delta W_{nc} = \delta\mathbf{q}^T[-q_f\hat{\mathbf{A}}\mathbf{q} + \hat{\mathbf{B}}_2 u(t) + \sqrt{r_w}\,\hat{\mathbf{B}}_{1d}\mathbf{w}_d(t)], \quad \mathbf{w}_d = col\{w_{di}\} \tag{11}$$

where the generalized coordinates are $\mathbf{q} = col_{\alpha,\beta}\{q_{\alpha\beta}\}$. Given the energy expressions and boundary conditions, it is readily verified that $\mathbf{M}$, $\mathbf{K}_b$, $\hat{\mathbf{K}}_0$, and $\hat{\mathbf{K}}_c$ are symmetric and positive-definite. Given the normalizations used for the basis functions, $\mathbf{M} = \mathbf{1}$. The gyroscopic matrix $\hat{\mathbf{G}}$ and the circulatory matrix $\hat{\mathbf{A}}$ are skew-symmetric. The control input matrix is given by $\hat{\mathbf{B}}_2 = col_{\alpha,\beta}\{\phi_\alpha(x_a)\psi_\beta(y_a)\}$ and the columns of $\hat{\mathbf{B}}_{1d}$ are of the same form with (x_a, y_a) replaced with (x_{di}, y_{di}). Space considerations prevent us from defining the remaining matrices in detail; however, their construction is relatively straightforward.

Forming the Lagrangian $L = T - U_b - U_s$ and applying Hamilton's (extended) principle to the energy expressions yields the equations of motion

$$\mathbf{M}\ddot{\mathbf{q}} + (\hat{\mathbf{D}} + c\hat{\mathbf{G}})\dot{\mathbf{q}} + [\mathbf{K} + q_c\hat{\mathbf{K}}_c + q_f\hat{\mathbf{A}}]\mathbf{q} = \hat{\mathbf{B}}_2 u(t) + \sqrt{r_w}\,\hat{\mathbf{B}}_{1d}\mathbf{w}_d(t) \tag{12}$$

where $\mathbf{K} = \mathbf{K}_b + q_0\hat{\mathbf{K}}_0$ and we have taken the liberty of adding a structural damping term, $\hat{\mathbf{D}}\dot{\mathbf{q}}$, whose construction is discussed below. Assumed to be available for control purposes is a single corrupted velocity measurement collocated with the control force input:

$$y(t) = \dot{w}(x_a, y_a, t) + \sqrt{r_v}\,w_s(t) = \hat{\mathbf{C}}_2\dot{\mathbf{q}} + \sqrt{r_v}\,w_s(t). \tag{13}$$

Here, $w_s(t)$ is sensor noise, $r_v > 0$ is a scaling, and $\hat{\mathbf{C}}_2 = \hat{\mathbf{B}}_2^T$ given the collocation assumption.

For the problem at hand, the number of basis functions employed is typically 50 ($n = 5$, $m = 10$). In order to design low-order controllers, the above equations can be transformed to modal coordinates and truncated. Let $\mathbf{E}$ be the normalized eigenmatrix corresponding to the nonmoving ($c = 0$), noncutting ($q_c = q_f = 0$) blade, i.e., $\mathbf{E}^T\mathbf{M}\mathbf{E} = \mathbf{1}$, $\mathbf{E}^T\mathbf{K}\mathbf{E} = \mathbf{\Omega}_0^2 = \text{diag}\ \{\omega_{0\alpha}^2\}$ where $\omega_{0\alpha}$ are the vibration frequencies for this case ($\mathbf{1}$ will denote the identity matrix of appropriate dimension). It is assumed that $\mathbf{E}^T\hat{\mathbf{D}}\mathbf{E} = \text{diag}\ \{2\zeta_{0\alpha}\omega_{0\alpha}\}$ where the $\zeta_{0\alpha}$ are modal damping factors relative to the tensioned frequencies. Partition this matrix into $\mathbf{E} = [\mathbf{E}_c \quad \mathbf{E}_r]$, where $\mathbf{E}_c$ denotes the first N_c modes to be retained for controller design. Substituting the truncated modal expansion $\mathbf{q}(t) = \mathbf{E}_c\hat{\mathbf{q}}(t)$ into Eq. (12) and premultiplying by $\mathbf{E}_c^T$ gives a reduced set of equations for $\hat{\mathbf{q}}$. They maintain the form of (12) with each square matrix $(\cdot)$ on the left-hand side replaced with $\mathbf{E}_c^T(\cdot)\mathbf{E}_c$. Similarly, the $\hat{\mathbf{B}}_{(\cdot)}$ matrices on the right-hand side are replaced with $\mathbf{E}_c^T\hat{\mathbf{B}}_{(\cdot)}$. The matrix $\hat{\mathbf{C}}_2$ in Eq. (13) is replaced with $\hat{\mathbf{C}}_2\mathbf{E}_c$. The original notation is used with the understanding that Eqs. (12) and (13) have been replaced by their reduced-order equivalents and $\mathbf{q}$ now refers to $\hat{\mathbf{q}}$.

The cutting force is assumed to consist of a nominal constant part and an (uncertain) time-varying component:

$$q_c(t) = q_f(t) = \bar{q}_c + \hat{q}_c\Delta_c(t) \tag{14}$$

where $|\Delta_c(t)| \le 1$, $0 \le t \le \infty$, and $\hat{q}_c$ is used to scale the size of the uncertainty. The motion equation (12) and the uncertainty model (14) can be used to form the first-order state-space model

$$\dot{\mathbf{x}} = \mathbf{A}\mathbf{x} + \mathbf{B}_{1p}\mathbf{w}_p(t) + \mathbf{B}_{1\Delta}\mathbf{w}_\Delta + \mathbf{B}_2\mathbf{u} \tag{15}$$

$$\mathbf{w}_\Delta = \mathbf{\Delta}(t)\mathbf{z}_\Delta(t), \quad \mathbf{\Delta} = \Delta_c\mathbf{1}, \quad 0 \le |\Delta_c(t)| \le 1 \tag{16}$$

$$\mathbf{z}_\Delta = \mathbf{C}_{1\Delta}\mathbf{x}(t), \quad \mathbf{C}_{1\Delta} = [\mathbf{O} \quad \hat{q}_c(\hat{\mathbf{K}}_c + \hat{\mathbf{A}})] \tag{17}$$

The following matrices have been introduced:

$$\mathbf{x} = \begin{bmatrix} \dot{\mathbf{q}} \\ \mathbf{q} \end{bmatrix}, \quad \mathbf{A} = \begin{bmatrix} -\hat{\mathbf{D}} - c\hat{\mathbf{G}} & -\mathbf{K} - \bar{q}_c(\hat{\mathbf{K}}_c + \hat{\mathbf{A}}) \\ \mathbf{1} & \mathbf{O} \end{bmatrix},$$

$$\mathbf{B}_{1\Delta} = \begin{bmatrix} \mathbf{1} \\ \mathbf{O} \end{bmatrix}, \quad \mathbf{B}_2 = \begin{bmatrix} \hat{\mathbf{B}}_2 \\ \mathbf{O} \end{bmatrix} \tag{18}$$

$$\mathbf{w}_p(t) = \begin{bmatrix} \mathbf{w}_d(t) \\ w_s(t) \end{bmatrix}, \quad \mathbf{B}_{1p} = [\mathbf{B}_{1d} \quad \mathbf{O}], \quad \mathbf{B}_{1d} = \begin{bmatrix} \sqrt{r_w}\,\hat{\mathbf{B}}_{1d} \\ \mathbf{O} \end{bmatrix}. \tag{19}$$

Consistent with this, the output equation (13) can be rewritten as

$$\mathbf{y} = \mathbf{C}_2\mathbf{x}(t) + \mathbf{D}_{2p1}\mathbf{w}_p, \quad \mathbf{C}_2 = [\hat{\mathbf{C}}_2 \quad \mathbf{O}],$$
$$\mathbf{D}_{2p1} = [\mathbf{0} \quad \sqrt{r_v}] \tag{20}$$

Notice that the time-varying parameters in (15)–(17) have been written in the so-called perturbation feedback format discussed by Doyle and Packard (1993).

In addition, the regulated outputs or performance variables are required, i.e., those which the controller must keep small:

$$\mathbf{z}_p(t) = \begin{bmatrix} \sqrt{q}\,\hat{\mathbf{C}}_{1p}\mathbf{x}(t) \\ \sqrt{r}\,u(t) \end{bmatrix} = \mathbf{C}_{1p}\mathbf{x}(t) + \mathbf{D}_{1p2}u(t),$$
$$\mathbf{C}_{1p} = \begin{bmatrix} \sqrt{q}\,\hat{\mathbf{C}}_{1p} \\ \mathbf{O} \end{bmatrix}, \quad \mathbf{D}_{1p2} = \begin{bmatrix} \mathbf{O} \\ \sqrt{r} \end{bmatrix} \tag{21}$$

Here, $q > 0$, $r > 0$ are scalings which allow one to tradeoff the relative importance of regulating the states and keeping control effort small. A suitable choice for $\hat{\mathbf{C}}_{1p}$ is diag $\{\mathbf{1}, \mathbf{\Omega}_0\}$ so that $\mathbf{x}^T\hat{\mathbf{C}}_{1p}^T\hat{\mathbf{C}}_{1p}\mathbf{x}/2$ would measure the energy in the nontranslating, noncutting case. It is assumed that $(\mathbf{A}, \mathbf{B}_{1p})$, $(\mathbf{A}, \mathbf{B}_{1\Delta})$, and $(\mathbf{A}, \mathbf{B}_2)$ are controllable pairs and $(\mathbf{C}_{1p}, \mathbf{A})$, $(\mathbf{C}_{1\Delta}, \mathbf{A})$, and $(\mathbf{C}_2, \mathbf{A})$ are observable pairs. These are readily satisfied for appropriate choices of actuator/sensor location (x_a, y_a) and disturbance locations (x_{di}, y_{di}), $i = 1 \ldots n_d$. The control problem can be roughly stated as follows: find a control system with input y and output u so as to provide system stability for all $\mathbf{\Delta}$ given by (16) and reduce the effect of $\mathbf{w}_p$ defined in (19) on $\mathbf{z}_p$ in (21).

3 Controller Design

The basic input-output notions required for the controller design are presented here. The reader may consult the book of Desoer and Vidyasagar (1975) for a more complete treatment. Consider a system $\mathbf{y}(t) = \boldsymbol{G}\mathbf{u}(t)$ where $\boldsymbol{G}$ is a (possibly time-varying and/or nonlinear) operator. The size of time signals can be established using their energy as measured by the L_2-norm:

$$\|\mathbf{u}\|_2^2 = \int_0^\infty \mathbf{u}^T\mathbf{u}\,dt, \quad L_2 = \{\mathbf{u} \,|\, \|\mathbf{u}\|_2 < \infty\}$$

A general system with input $\mathbf{u}(t)$ and output $\mathbf{y}(t) = \boldsymbol{G}\mathbf{u}$ is L_2-stable if there exists K, $0 < K < \infty$, such that $\|\mathbf{y}\|_2 \le K\|\mathbf{u}\|_2$, $\forall \mathbf{u} \in L_2$. The smallest such value of K is the gain of the system which can also be defined as

$$\|\boldsymbol{G}\| = \sup_{\mathbf{0}\neq\mathbf{u}\in L_2} \frac{\|\boldsymbol{G}\mathbf{u}\|_2}{\|\mathbf{u}\|_2} \tag{22}$$

which measures the worst-case energy gain over all finite energy inputs.

If $\boldsymbol{G}$ corresponds to the linear time-invariant (LTI) system

$$\mathbf{y}(t) = \mathbf{C}\mathbf{x} + \mathbf{D}\mathbf{u}, \quad \dot{\mathbf{x}} = \mathbf{A}\mathbf{x} + \mathbf{B}\mathbf{u}(t) \tag{23}$$

then Laplace transforms can be used to write $\mathbf{y}(s) = \mathbf{G}(s)\mathbf{u}(s)$ where the transfer matrix $\mathbf{G}(s)$ is given by

$$\mathbf{G}(s) = \left[\begin{array}{c|c} \mathbf{A} & \mathbf{B} \\ \hline \mathbf{C} & \mathbf{D} \end{array}\right] \stackrel{\triangle}{=} \mathbf{C}(s\mathbf{1} - \mathbf{A})^{-1}\mathbf{B} + \mathbf{D}$$

(The notational convention of Doyle et al. (1989) has been adopted.) In this case, the system gain is the $\mathcal{H}_\infty$-norm of the transfer matrix:

$$\|\boldsymbol{G}\| = \|\mathbf{G}(s)\|_\infty = \sup_{\omega\in[0,\infty]} \sigma_{\max}[\mathbf{G}(j\omega)] \tag{24}$$

where $\sigma_{\max}$ denotes the largest singular value. If the system (23) is controllable and observable then $\|\mathbf{G}\|_\infty < \infty$ is equivalent to the eigenvalues of $\mathbf{A}$ having negative real parts. For a linear time-varying system $\mathbf{y}(t) = \boldsymbol{G}\mathbf{u}(t)$, $\|\boldsymbol{G}\| < \infty$ implies global asymptotic stability for the unforced ($\mathbf{u} = \mathbf{0}$) state representation of the system under the same assumptions. The introduction of the norm in (22) permits a framework that can simultaneously handle performance and stability considerations for time-varying systems.

Another norm for measuring the size of $\mathbf{G}(s)$ is the $\mathcal{H}_2$-norm:

$$\|\mathbf{G}\|_2^2 = \frac{1}{2\pi}\int_{-\infty}^{\infty} \text{trace}\,\{\mathbf{G}^H(j\omega)\mathbf{G}(j\omega)\}d\omega \tag{25}$$

When $\mathbf{D} = \mathbf{O}$ in (23), this can be interpreted as the expected value of

$$\lim_{T\to\infty}\frac{1}{T}\int_0^T \mathbf{y}^T\mathbf{y}\,dt$$

when $\mathbf{u}(t)$ is zero-mean, unit intensity, Gaussian white noise.

Now consider the block diagram corresponding to the system described by (15)–(21):

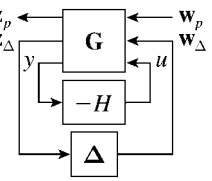

$$\mathbf{G}(s) = \left[\begin{array}{c|ccc} \mathbf{A} & \mathbf{B}_{1p} & \mathbf{B}_{1\Delta} & \mathbf{B}_2 \\ \hline \mathbf{C}_{1p} & \mathbf{O} & \mathbf{O} & \mathbf{D}_{1p2} \\ \mathbf{C}_{1\Delta} & \mathbf{O} & \mathbf{O} & \mathbf{O} \\ \mathbf{C}_2 & \mathbf{D}_{2p1} & \mathbf{O} & \mathbf{O} \end{array}\right] \tag{26}$$

It has been assumed that $y(t)$ and $u(t)$ are related by an LTI system H, i.e., $y(s) = -H(s)u(s)$ where $H(s)$ is a stabilizing controller to be determined. Let $\mathcal{T}_{z_pw_p}(H, \mathbf{\Delta})$ denote the closed-loop operator from $\mathbf{w}_p(t)$ to $\mathbf{z}_p(t)$. When $\mathbf{\Delta} = \mathbf{O}$, the closed-loop system can be represented by the transfer matrix

$$\begin{bmatrix} \mathbf{z}_p \\ \mathbf{z}_\Delta \end{bmatrix} = \mathbf{T}_{zw}(s)\begin{bmatrix} \mathbf{w}_p \\ \mathbf{w}_\Delta \end{bmatrix}, \quad \mathbf{T}_{zw}(s) = \begin{bmatrix} \mathbf{T}_{z_pw_p}(s) & \mathbf{T}_{z_pw_\Delta}(s) \\ \mathbf{T}_{z_\Delta w_p}(s) & \mathbf{T}_{z_\Delta w_\Delta}(s) \end{bmatrix} \tag{27}$$

Hence, $\mathbf{T}_{z_pw_p}(s)$ is the transfer matrix corresponding to $\mathcal{T}_{z_pw_p}(H, \mathbf{O})$.

The following control problems for the bandsaw problem will be solved:

I. $\mathcal{H}_2$-Nominal Performance. Find $H(s)$ so as to minimize $\|\mathbf{T}_{z_pw_p}\|_2$. This is the standard Linear-Quadratic-Gaussian (LQG) problem and is equivalent to minimizing the expected value of

$$\mathcal{J} = \lim_{T\to\infty}\frac{1}{T}\int_0^T [q\mathbf{x}^T\mathbf{C}_{1p}^T\mathbf{C}_{1p}\mathbf{x} + ru^2(t)]dt$$

subject to (15) and (20) under the assumption that $\mathbf{w}_\Delta = \mathbf{0}$ and $\mathbf{w}_p(t)$ is a zero-mean, unit intensity, Gaussian white noise process. This standard problem is used to determine reasonable values for the weighting parameters q, r, r_w, and r_v. This is assessed by examination of the closed-loop eigenvalues which should exhibit reasonable damping and estimator speed. The values of q and r were also scaled so that $\|\mathbf{T}_{z_pw_p}\|_\infty$ for this design was on the order of unity.

II. $\mathcal{H}_\infty$-Nominal Performance. Find $H(s)$ so as to minimize $\|\mathbf{T}_{z_p w_p}\|_\infty$. In general, this problem is solved by finding an $H(s)$ which makes $\|\mathbf{T}_{z_p w_p}\|_\infty < \gamma$, and systematically reducing γ until no solution is possible.

III. Robust Stability. Find $H(s)$ so that the perturbed system is L_2-stable, i.e., $\|\mathcal{T}_{z_p w_p}(H, \mathbf{\Delta})\| < \infty$ for all linear time-varying (LTV) $\mathbf{\Delta}$ such that $\|\mathbf{\Delta}\| \leq 1$. Necessary and sufficient conditions are as follows:

$$\|\mathbf{T}_{z_\Delta w_\Delta}\|_\infty < \gamma = 1 \tag{28}$$

The sufficiency of this result is an instance of the multivariable circle criterion reported by Safanov and Athans (1981). The necessity in this case means that if $\|\mathbf{T}_{z_\Delta w_\Delta}\|_\infty = 1$, then there exists a linear time-varying $\mathbf{\Delta}$ with $\|\mathbf{\Delta}\| \leq 1$ which leads to instability (Shamma, 1994). Note that if (28) holds then stability is guaranteed for any LTV $\mathbf{\Delta}$ satisfying the norm bound regardless of structure. This is a larger class of perturbations than that defined by (15) but leads to a robust performance problem that is analytically tractable. It also allows for additional unmodeled dynamics in the cutting-force loop. By determining the smallest value of γ such that (28) is satisfied (call it γ_{opt}), one can enlarge the class of stabilizing perturbations to $\|\mathbf{\Delta}\| \leq \gamma_{\text{opt}}^{-1}$.

IV. Robust Performance. Find $H(s)$ so that the system is L_2-stable and achieves the performance criterion $\|\mathcal{T}_{z_p w_p}(H, \mathbf{\Delta})\| < \gamma$ for all LTV $\mathbf{\Delta}$ such that $\|\mathbf{\Delta}\| \leq \gamma^{-1}$. Necessary and sufficient conditions are as follows: there exists a constant matrix $\mathbf{D}$ of the form

$$\mathbf{D} = \begin{bmatrix} \mathbf{1} & \mathbf{O} \\ \mathbf{O} & d\mathbf{1} \end{bmatrix}, \quad d > 0 \tag{29}$$

such that

$$\|\mathbf{D}^{-1}\mathbf{T}_{zw}(s)\mathbf{D}\|_\infty < \gamma \tag{30}$$

where $\mathbf{T}_{zw}$ is defined by (27). This result has been derived by Shamma (1994) and Poolla and Tikku (1995). The presence of the constant scaling matrix $\mathbf{D}$ essentially leads to the following substitutions: $\mathbf{B}_{1\Delta} \rightarrow d\mathbf{B}_{1\Delta}$ and $\mathbf{C}_{1\Delta} \rightarrow d^{-1}\mathbf{C}_{1\Delta}$. The solution of problem IV is then equivalent to solving a standard linear time-invariant $\mathcal{H}_\infty$ control problem. To this end, define

$$\mathbf{B}_1 = [\mathbf{B}_{1p} \quad d\mathbf{B}_{1\Delta}], \quad \mathbf{C}_1^T = [\mathbf{C}_{1p}^T \quad d^{-1}\mathbf{C}_{1\Delta}^T] \tag{31}$$

The solution of all four problems can be tackled using the same framework wherein the solutions of problems I–III become special cases of that of problem IV. Using the state-space solutions reported by Doyle et al. (1989), a controller satisfying (30) for general γ (if it exists) has the form

$$H(s) = \left[\begin{array}{c|c} \mathbf{A}_c & \mathbf{K}_e \\ \hline \mathbf{K}_c & \mathbf{O} \end{array}\right] \Rightarrow$$

$$u(t) = -\mathbf{K}_c\mathbf{x}_c(t), \quad \dot{\mathbf{x}}_c = \mathbf{A}_c\mathbf{x}_c + \mathbf{K}_e y(t). \tag{32}$$

The matrices $(\mathbf{A}_c, \mathbf{K}_c, \mathbf{K}_e)$ are given by

$$\mathbf{K}_c = r^{-1}\mathbf{B}_2^T\mathbf{X}, \quad \mathbf{K}_e = \mathbf{ZYC}_2^T r_v^{-1} \tag{33}$$

$$\mathbf{A}_c = \mathbf{A} - \mathbf{B}_2\mathbf{K}_c - \mathbf{K}_e\mathbf{C}_2 + \gamma^{-2}\mathbf{B}_1\mathbf{B}_1^T\mathbf{X} \tag{34}$$

Here, $\mathbf{Z} = (\mathbf{1} - \gamma^{-2}\mathbf{YX})^{-1}$ and $\mathbf{X}$ and $\mathbf{Y}$ are solutions of the algebraic Riccati equations:

$$\mathbf{XA} + \mathbf{A}^T\mathbf{X} - \mathbf{XS}_x\mathbf{X} + \mathbf{Q}_x = \mathbf{O} \tag{35}$$

$$\mathbf{AY} + \mathbf{YA}^T - \mathbf{YS}_y\mathbf{Y} + \mathbf{Q}_y = \mathbf{O} \tag{36}$$

where

$$\mathbf{S}_x = r^{-1}\mathbf{B}_2\mathbf{B}_2^T - \gamma^{-2}\mathbf{B}_1\mathbf{B}_1^T, \quad \mathbf{Q}_x = \mathbf{C}_1^T\mathbf{C}_1 \tag{37}$$

$$\mathbf{S}_y = r_v^{-1}\mathbf{C}_2^T\mathbf{C}_2 - \gamma^{-2}\mathbf{C}_1^T\mathbf{C}_1, \quad \mathbf{Q}_y = \mathbf{B}_1\mathbf{B}_1^T \tag{38}$$

Table 1 Bandsaw parameters

$\rho = 8200\,kg{\cdot}m^{-3}$	$\ell = 0.8\,m$	$b = 0.22\,m$	$h = 1.65\,mm$
$c = -40\,m/s$	$D = 18.1\,N{\cdot}m$	$\nu = 0.3$	$q_0 = 68\,kN/m$
$\zeta_{0\alpha} = 0.05$	$N_c = 5$	$x_a = 0.4a$	$y_b = 0.2b$

and from (31),

$$\mathbf{B}_1\mathbf{B}_1^T = \mathbf{B}_{1p}\mathbf{B}_{1p}^T + d^2\mathbf{B}_{1\Delta}\mathbf{B}_{1\Delta}^T,$$

$$\mathbf{C}_1^T\mathbf{C}_1 = \mathbf{C}_{1p}^T\mathbf{C}_{1p} + d^{-2}\mathbf{C}_{1\Delta}^T\mathbf{C}_{1\Delta}. \tag{39}$$

Hence, problem IV is solved by fixing d and attempting to solve the Riccati equations (35) and (36). In order for condition (30) to be satisfied by a stabilizing compensator, (35) and (36) must have unique positive-semidefinite solutions and the following condition must be satisfied:

$$\rho(\mathbf{XY}) < \gamma^2 \tag{40}$$

where $\rho(\cdot)$ denotes the spectral norm.

For problem I, the $\mathcal{H}_2$-optimal (LQG) solution is obtained by letting $\gamma \rightarrow \infty$ in Eqs. (33)–(38) and ignoring all terms containing the subscript Δ in Eq. (39). Under the controllability and observability hypotheses that have been made, a unique solution for $\mathbf{X}$ and $\mathbf{Y}$ exists and the controller (32) stabilizes the nominal ($\mathbf{\Delta} = \mathbf{O}$) system. Note that $\mathbf{Z} = \mathbf{1}$ in this case.

For problem II, the $\mathcal{H}_\infty$ (sub-) optimal solution is given by the above and requires that the Riccati equations (35) and (36) have unique positive-semidefinite solutions and (40) is satisfied. Again, one ignores the Δ-terms in (39). Using the controller (32), the two transfer matrices on the diagonal in (27) are given by

$$\mathbf{T}_{z_p w_p}(s) = \left[\begin{array}{cc|c} \mathbf{A} & -\mathbf{B}_2\mathbf{K}_c & \mathbf{B}_{1p} \\ \mathbf{K}_e\mathbf{C}_2 & \mathbf{A}_c & \mathbf{K}_e\mathbf{D}_{2p1} \\ \hline \mathbf{C}_{1p} & -\mathbf{D}_{1p2}\mathbf{K}_c & \mathbf{O} \end{array}\right],$$

$$\mathbf{T}_{z_\Delta w_\Delta}(s) = \left[\begin{array}{cc|c} \mathbf{A} & -\mathbf{B}_2\mathbf{K}_c & \mathbf{B}_{1\Delta} \\ \mathbf{K}_e\mathbf{C}_2 & \mathbf{A}_c & \mathbf{O} \\ \hline \mathbf{C}_{1\Delta} & \mathbf{O} & \mathbf{O} \end{array}\right]. \tag{41}$$

The optimal solution of problem II minimises the $\mathcal{H}_\infty$-norm of the first transfer matrix.

Problem III is also an $\mathcal{H}_\infty$-optimization and can be solved using Eqs. (32)–(40) but this time with $\mathbf{B}_{1p} = \mathbf{C}_{1p} = \mathbf{O}$, $d = 1$ in (39) and $r = r_v = \epsilon > 0$ (a small number) so that $\|\mathbf{T}_{zw}\|_\infty \doteq \|\mathbf{T}_{z_\Delta w_\Delta}\|_\infty$. In this case, the smallest γ for which (28) is satisfied yields optimal stability robustness, i.e., the largest uncertainty set for which stabilization by an LTI controller is possible. It minimises the $\mathcal{H}_\infty$-norm of the second transfer matrix in (41). Experience has shown that the optimal form of this problem behaves very poorly from a numerical standpoint; only the solution for $\gamma = 1$ will be presented.

Alternatively, one can analyse any controller of the form (32) for robustness by calculating the maximum singular value of the transfer matrix $\mathbf{T}_{z_\Delta w_\Delta}$ in (41). Also note that nominal ($\mathbf{\Delta} = \mathbf{O}$) stability for all four control problems is governed by the eigenvalues of the composite "$\mathbf{A}$" matrix in (41), i.e., the upper 2×2 partition in each transfer matrix which is designated $\bar{\mathbf{A}}$ in the sequel.

4 Numerical Example

The controller synthesis is now applied to the model previously developed for the bandsaw blade. The system parameters introduced in Section 2 are given in Table 1 and are typical of wide bandsaws used for cutting timber. Note that the direction of motion is opposite to the sense of the cutting force on the blade. Although

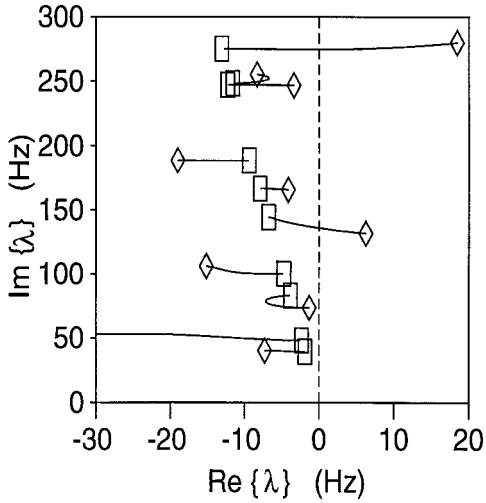

Fig. 2 Eigenloci for varying $q_c = q_f = \bar{q}_c$ (□ $\bar{q}_c = 0$, ◇ $\bar{q}_c = 50$ kN/m)

controllers will be designed later on the basis of a five mode model, illustrations of the plant behavior will be conducted using a ten mode "full order" model.

In order to motivate the controller design approach, the eigenvalues of **A** in (18) will be examined. Under noncutting conditions, $\bar{q}_c = 0$, and the circulatory matrix $\hat{\mathbf{A}}$ can be ignored. In this case, it is well known that the eigenvalues of **A** are purely imaginary (in the absence of damping) since the equivalent second-order system in (12) is a statically-stable gyroscopic system. The eigenvalues as a function of $q_c = q_f = \bar{q}_c$ are shown in Fig. 2 for a damping ratio of $\zeta_{0\alpha} = 0.05$ in all modes. It is clear that the nonconservative nature of the cutting force destabilizes the fifth and tenth vibration modes and eventually the third one.

The simplest controller that can be used is a constant gain rate feedback: $u(t) = -K_d y(t)$. This effectively adds a term $(-K_d \mathbf{B}_2 \mathbf{C}_2)$ to the **A** matrix. It can be readily shown that with $q_f = 0$, this matrix is guaranteed to have negative real eigenvalues for all possible (constant) values of the system parameters ρ, D, c, $\zeta_{0\alpha}$, q_0, and q_c when $q_f = 0$. A simple proof uses $T + U_b + U_s$ as a Lyapunov function. However, with $q_f = q_c = \bar{q}_c = 50$ kN/m, one obtains the eigenloci shown in Fig. 3 as a function of K_d. Stabilization is not possible for any K_d but for smaller values of $\bar{q}_c$ there is a limited range of values for which all ten modes are stabilized but the degree of damping added is limited.

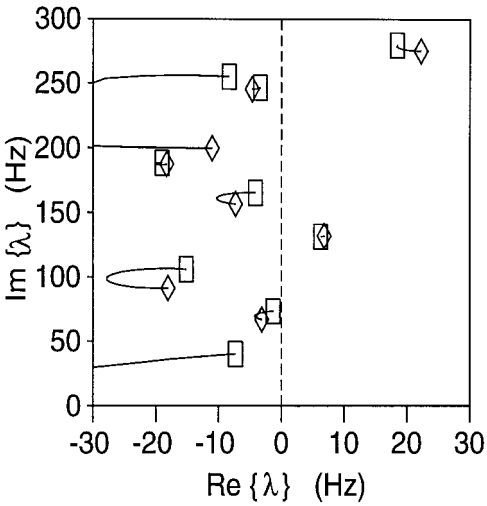

Fig. 3 Eigenloci for varying K_d ($q_c = q_f = 50$ kN/m) (□ $K_d = 0$, ◇ $K_d = 4$ kN/m/s)

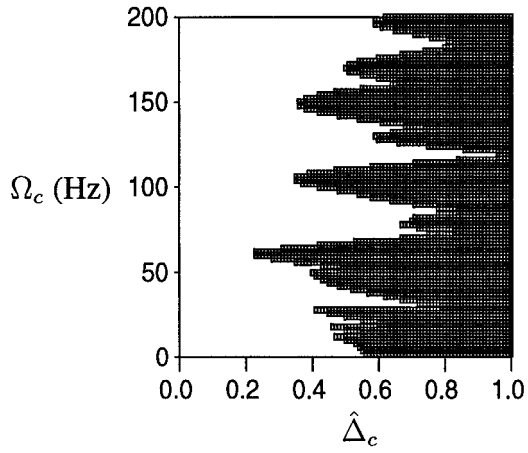

Fig. 4 Instability regions for Ω_c vs. $\hat{\Delta}_c$ ($\bar{q}_c = \hat{q}_c = 30$ kN/m, open-loop system) (□□ = unstable)

Now consider the unforced time-varying system in (15)–(17) with an assumed sinusoidal behavior for the cutting force, i.e., $\Delta_c(t) = \hat{\Delta}_c \sin \Omega t$, so that

$$\dot{\mathbf{x}} = (\mathbf{A} + \mathbf{B}_{1\Delta}\mathbf{C}_{1\Delta}\hat{\Delta}_c \sin \Omega_c t)\mathbf{x}. \tag{42}$$

The stability of this periodic system can be assessed using Floquet theory. Experience has shown that a numerically more reliable determination is possible using the method of harmonic balance. With this technique, a solution of the form

$$\mathbf{x}(t) = e^{\lambda t}[\mathbf{x}_0 + \sum_{i=1}^{N_b} (\mathbf{x}_{ci} \cos i\Omega t + \mathbf{x}_{si} \sin i\Omega t)]$$

is assumed which upon substitution into (42) produces a standard eigenproblem of dimension $(2N_b + 1)$ times greater than that corresponding to **A** alone. Stability of the time-varying system is then determined by examining the real parts of each λ. A stability diagram for various values of Ω_c and $\hat{\Delta}_c$ is shown in Fig. 4 for the case where $q_f = 0$, i.e., the follower-force effect is neglected, but $q_c(t) = \bar{q}_c + \hat{q}_c \Delta_c(t)$, with $\bar{q}_c = \hat{q}_c = 30$ kN/m. A value of $N_b = 2$ proved to be sufficient. If $q_f(t) = q_c(t)$, then the entire region illustrated in Fig. 4 was unstable which is not unexpected given the destabilization exhibited in Fig. 2 for constant $q_f = q_c$.

The sequence of control problems in the previous section is now treated with a view to obtaining satisfactory performance in the face of the time-varying follower-force nature of $q_f = q_c$. The controller design parameters are given in Table 2 and the first five mode shapes of the (damped) open-loop system under cutting conditions are shown in Fig. 5. The design parameters were chosen in such a way that the closed-loop system using the ten mode model was stable for all four controllers, i.e., spillover instabilities were avoided. In case II, we present results for the optimal case. In case III, a suboptimal solution for $\gamma = 1$ is presented. In case IV, a search over d was made to determine whether a solution existed for $\gamma = 1$. This was not the case, so results are presented for $d = 2$ and $\gamma = 2$. Graphs of $\sigma_{\max}[\mathbf{T}_{z_{p w_p}}(j\omega)]$ and $\sigma_{\max}[\mathbf{T}_{z_\Delta w_\Delta}(j\omega)]$ vs. ω are given in Figs. 6 and 7 for each controller relative to the design model ($N_c = 5$) and in

Table 2 Controller design parameters

i	x_{di}/ℓ	y_{di}/b	Design Parameters	
1	0.2	1.0	$q = 200$	$r = 0.2$
2	0.3	1.0	$r_w = 1$	$r_v = 1 \times 10^{-5}$
3	0.8	1.0	$\hat{q}_c = \bar{q}_c = 7.5\,kN/m$	$n_d = 3$

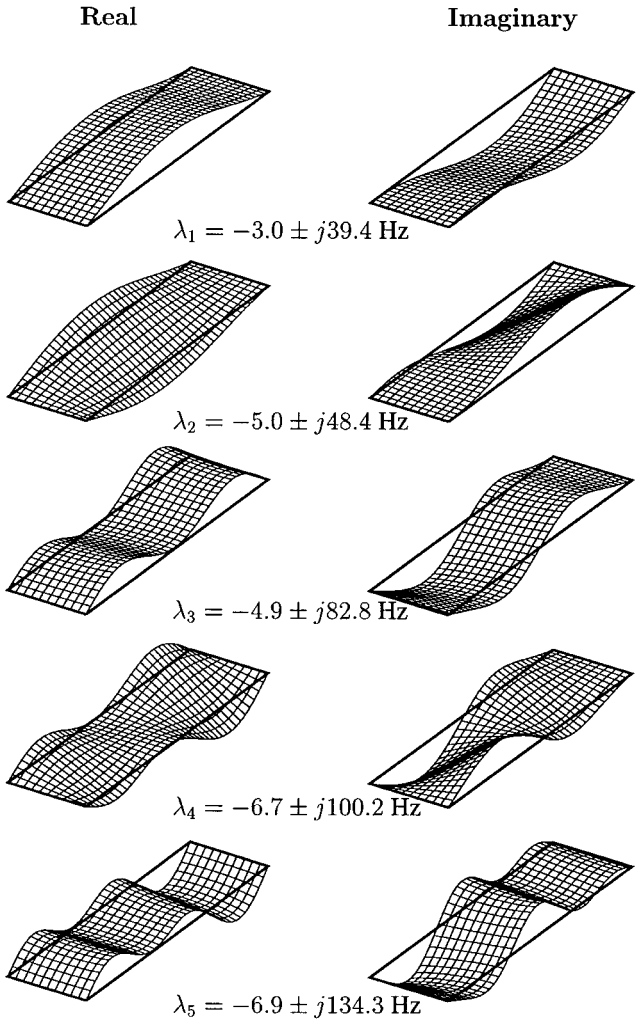

Fig. 5 The first five modes under cutting conditions

Figs. 8 and 9 relative to the full order plant. The Bode plots for $H(s)$ in each case are given in Fig. 10. The corresponding norms are collected in Table 3.

Controllers I and II yield the best performance for the design model in the relevant norm but fail to meet the robustness specification. The optimal $\mathcal{H}_\infty$-design shows only a marginal improvement over the LQG design but is more robust. Controller III yields close to optimal robustness and provides stability for all $\|\mathbf{\Delta}\| < 1/0.569$ and hence $|\Delta_c(t)| < 1.76$. For $\mathbf{\Delta}$ exceeding this bound, no LTI controller can be found which stabilizes the entire perturbation set. Also, note that performance of this robust controller as measured by $\|\mathbf{T}_{z_p w_p}\|_\infty$ is degraded somewhat. In case IV, the correct trade-off is achieved and both nominal performance and robustness specifications are achieved. For $d = 2$, the requirement in (30) was achieved for $\gamma = 2$ yielding robust performance for a

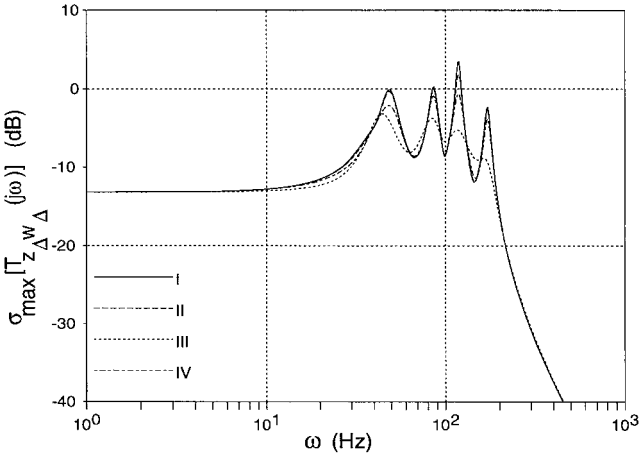

Fig. 7 Maximum singular values of $T_{z_\Delta w_\Delta}(j\omega)$ (5 mode plant model)

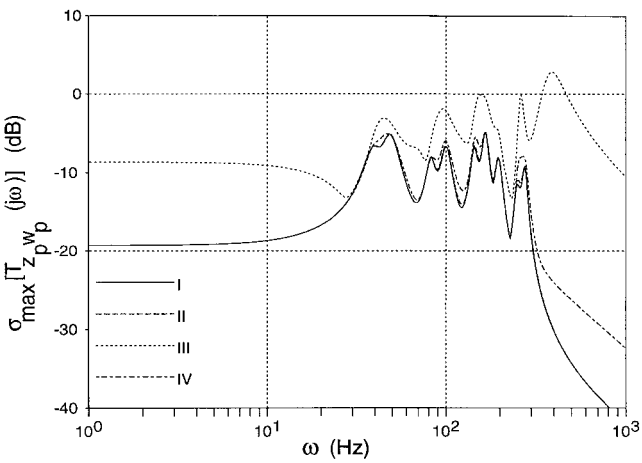

Fig. 8 Maximum singular values of $T_{z_p w_p}(j\omega)$ (10 mode plant model)

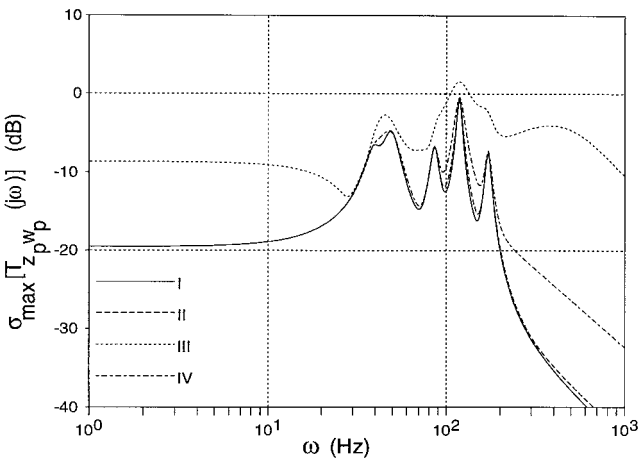

Fig. 6 Maximum singular values of $T_{z_p w_p}(j\omega)$ (5 mode plant model)

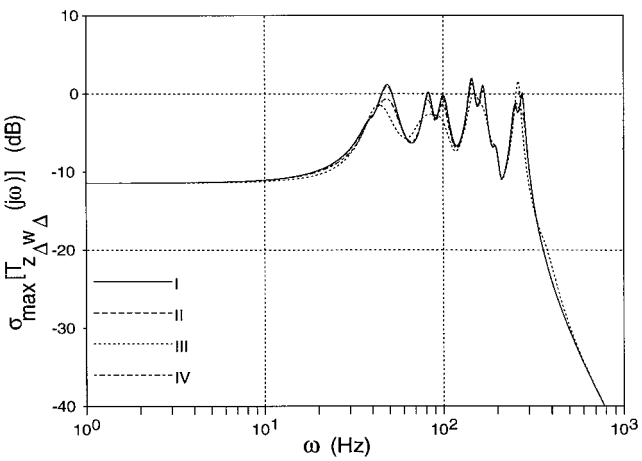

Fig. 9 Maximum singular values of $T_{z_\Delta w_\Delta}(j\omega)$ (10 mode plant model)

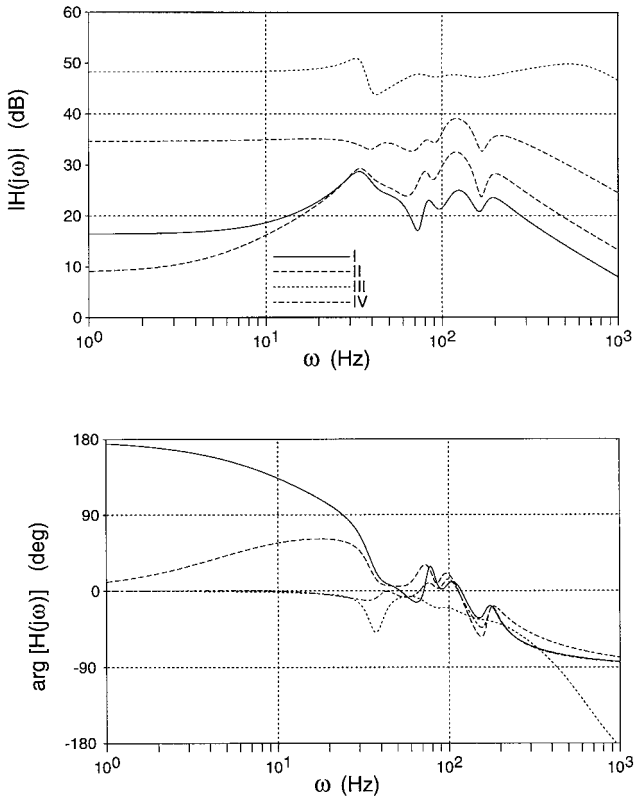

Fig. 10 Bode plots for *H*(*s*), controller designs I–IV

reduced specification. The singular value plots in Figs. 6 and 7 show that this controller closely achieves the performance levels of cases I and II but recovers some of the stability robustness characteristics of case III.

When the $\mathcal{H}_\infty$ performance measure was calculated relative to the full-order model, the relative ordering was preserved but the actual values in Table 3 were smaller. The corresponding stability robustness measure was also smaller in each case and controller IV outperformed the "optimal" robustness controller. A glance at Fig. 9 shows that the latter controller lost robustness at around 250 Hz owing to spillover.

The Bode plots in Fig. 10 yield great insight into the controllers. The $\mathcal{H}_\infty$ designs in cases II and IV have yielded a strictly positive real controller (the phase lies strictly in the range [−90 deg, 90 deg]) which is robustly stable with respect to (constant) perturbations of all quantities in Table 1 when $q_f = 0$. This follows from collocation of force actuation and rate sensing. The optimal $\mathcal{H}_\infty$ design in case II is close in form to the LQG design with some reduction in gain at low frequency. The robust designs in cases III and IV more closely approximate a constant rate gain at low frequency and at higher frequencies case IV acquires the characteristics of the higher performance controllers. The order of all controllers is the same as that of the plant model, namely $2N_c = 10$.

Table 3 Controller design summary

Type	$\|\|\mathbf{T}_{z_p w_p}\|\|_2$	$\|\|\mathbf{T}_{z_p w_p}\|\|_\infty$	$\|\|\mathbf{T}_{z_\Delta w_\Delta}\|\|_\infty$
	5 mode plant model		
I	7.17	0.941	1.51
II	7.38	0.893	1.24
III	28.0	1.20	0.69
IV	8.80	0.951	0.93
	10 mode plant model		
I	8.29	0.571	1.26
II	8.42	0.571	1.24
III	33.4	0.988	1.21
IV	9.48	0.579	1.16

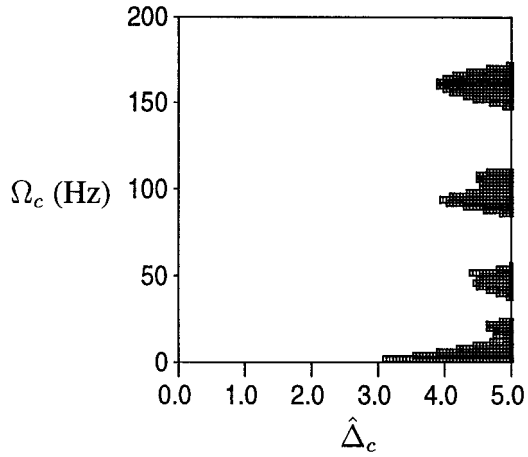

Fig. 11 Instability regions for Ω_c vs. $\hat{\Delta}_c$ ($\bar{q}_c = \hat{q}_c$ = 7.5 kN/m, controller IV) (□□ = unstable)

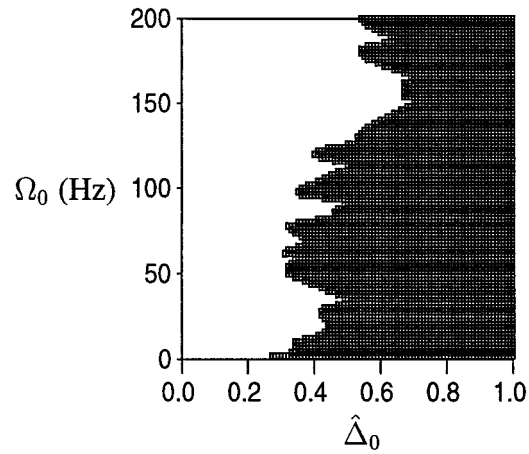

Fig. 12 Instability regions for Ω_0 vs. $\hat{\Delta}_0$ ($\bar{q}_0 = \hat{q}_0$ = 68 kN/m, q_c = 7.5 kN/m, controller IV) (□□ = unstable)

To illustrate the conservative nature of these designs with respect to the memoryless, diagonal form of the uncertainty in Eq. (16), consider the closed-loop system $\mathcal{T}(H, \mathbf{\Delta})$ with $\mathbf{\Delta} = \mathbf{1}\hat{\Delta}_c \sin \Omega t$. Stability can be determined by applying the method of harmonic balance to the system formed by wrapping $\mathbf{\Delta}$ in feedback around the transfer matrix $\mathbf{T}_{z_\Delta w_\Delta}$ in Eq. (41). The unforced form is of the same general form as (42) with $\mathbf{A}$ replaced with $\bar{\mathbf{A}}$ and $\mathbf{B}_{1\Delta}$, $\mathbf{C}_{1\Delta}$ replaced with the augmented forms in (41). The resulting stability diagram is given in Fig. 11 for controller design IV using the cutting force parameters in Table 2. Unlike Fig. 4 which was generated by ignoring the follower-force effect ($q_f = 0$), Fig. 11 was created assuming $q_f(t) = q_c(t) = \bar{q}_c + \hat{q}_c \Delta_c(t)$. Notice that

Table 4 External signals for simulation

Signal	Description	Freq., f (Hz)
$w_s(t)$	$\sin 2\pi f_s t$	50
$\mathbf{w}_d(t)$	$100\,[1\ 1\ 1]^T \sin 2\pi f_d t$	85
$\hat{\Delta}_c(t)$	$0.5 \sin 2\pi f_c t$	40
$\hat{\Delta}_0(t)$	$0.15 \sin 2\pi f_0 t$	15

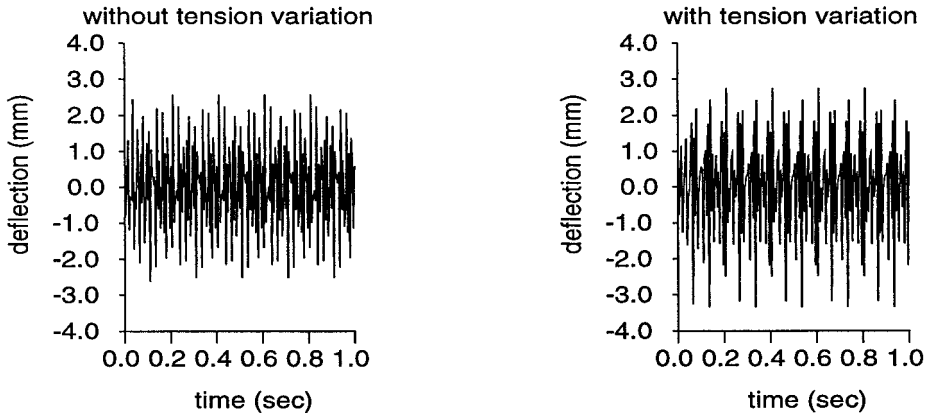

Fig. 13 Simulation results for sinusoidal disturbances and parameter variation

stability is guaranteed for $0 \leq |\Delta_c(t)| \leq 3.1$ when $\Delta_c(t)$ is restricted to being periodic.

The previous results have assumed that the blade tension, q_0, was constant. In practice, this will also vary and it is important that the controller exhibit robustness with respect to these variations. To this end consider $q_0(t) = \bar{q}_0(1 + \hat{\Delta}_0 \sin \Omega_0 t)$ with $\bar{q}_0$ assuming the nominal value. Stability in this case can be tested as above using the method of harmonic balance. Here, the nontrivial partition in $\mathbf{C}_{1\Delta}$ in Eq. (17) must be replaced with $\bar{q}_0\hat{\mathbf{K}}_0$. The resulting stability diagram developed using controller IV is given in Fig. 12 and demonstrates stability robustness with respect to tension variations within ± 25 percent. The time domain behavior of the closed-loop system can be gaged by simulating Eqs. (12) and (13) with the loop closed using controller IV. The sensor noise ($w_s(t)$), the blade disturbance ($\mathbf{w}_d(t)$), and the temporal variations in the cutting force and blade tension, are taken to be sinusoidal signals with the characteristics given in Table 4. The closed-loop behavior of the blade deflection at the sensor location (x_a, y_a) is shown in Fig. 13 with and without tension variation.

5 Concluding Remarks

An analytical study has been presented which shows how recent advances in robust control theory can be used to suppress unwanted bandsaw vibrations. The single-input/single-output LTI controllers presented achieve prescribed performance bounds and stability with respect to a family of time-varying perturbations which also exhibit follower-force behavior. Future work will address controller development for more complicated uncertainty descriptions (time-varying cutting force and blade tension) as well as experimental implementation. Current research focuses on the development of suitable noncontacting force actuation.

References

Alspaugh, G., 1967, "Torsional Vibration of a Moving Band," *J. Franklin Institute*, Vol. 283, pp. 328–338.

Bhat, R. B., 1985, "Natural Frequencies of Rectangular Plates Using Characteristic Orthogonal Polynomials in the Rayleigh-Ritz Method," *J. Sound and Vibration*, Vol. 102, No. 4, pp. 493–499.

Desoer, C. A., and Vidyasagar, M., 1975, *Feedback Systems: Input-Output Properties*, Academic Press, New York.

Doyle, J. C., Glover, K., Khargonekar, P. P., and Francis, B. A., 1989, "State-Space Solutions to Standard H_2 and H_∞ Control Problems," *IEEE Trans. Automatic Control*, Vol. 34, No. 8, pp. 831–847.

Lehmann, B. F., and Hutton, S. G., 1996, "The Mechanics of Bandsaw Cutting, Pt. I," *Holz als Roh- und Werkstoff*, Vol. 54, pp. 423–428.

Lehmann, B. F., and Hutton, S. G., 1997, "The Mechanics of Bandsaw Cutting, Pt. II," *Holz als Roh- und Werkstoff*, Vol. 55, pp. 35–43.

Lengoc, L., and McCallion, H., 1995, "Wide Bandsaw Blade Under Cutting Conditions, Part I: Vibration of a Plate Moving in its Plane While Subjected to Tangential Edge Loading; Part II: Stability of a Plate Moving in its Plane while Subjected to Parametric Excitation; Part III: Stability of a Plate Moving in its Plane While Subjected to Non-conservative Cutting Forces," *J. Sound and Vibration*, Vol. 186, No. 1, pp. 125–142, 143–162, 163–179.

Mote, C. D., Jr., and Naguleswaran, S., 1966, "Theoretical and Experimental Band Saw Vibrations," ASME *Journal of Engineering for Industry*, Vol. 88, pp. 151–156.

Naguleswaran, S., and Williams, C., 1968, "Lateral Vibration of Bandsaw Blades, Pulley Belts, and the Like," *Int. J. of Mechanical Sciences*, Vol. 10, pp. 239–250.

Packard, A., and Doyle, J., 1993, "The Complex Structured Singular Value," *Automatica*, Vol. 29, No. 1, pp. 71–109.

Poolla, K., and Tikku, A., 1995, "Robust Performance Against Time-Varying Structured Perturbations," *IEEE Trans. Automatic Control*, Vol. 40, No. 9, pp. 1589–1602.

Safonov, M. G., and Athans, M., 1981, "A Multiloop Generalization of the Circle Criterion for Stability Margin Analysis," *IEEE Trans. Automatic Control*, Vol. 26, No. 2, pp. 415–422.

Shamma, J. S., 1994, "Robust Stability with Time-Varying Structured Uncertainty," *IEEE Trans. Automatic Control*, Vol. 39, No. 4, pp. 714–724.

Soler, J., 1968, "Vibrations and Stability of a Moving Band," *J. Franklin Institute*, Vol. 286, pp. 295–307.

Ulsoy, A. G., and Mote, C. D., Jr., 1982, "Vibration of Wide Bandsaw Blades," ASME *Journal of Engineering for Industry*, Vol. 104, pp. 71–78.